IOP Conf. Series: Journal of Physics: Conf. Series **844** (2017) 012056 doi:10.1088/1742-6596/844/1/012056

Amplified spontaneous emission of an end-pumped cesium vapor laser

Guofei An, You Wang*, He Cai, Juhong Han, Shunyan Wang, Kepeng Rong, Hang Yu, Liangping Xue, Wei Zhang, Hongyuan Wang, and Jie Zhou

Southwest Institute of Technical Physics, Chengdu, Sichuan 610041, China

youwang_2007@aliyun.com

Abstract. Diode pumped alkali lasers (DPALs) provide a significant potential for construction of high-powered lasers. A series of models have been established to analyze the DPAL's kinetic process and most of them are based on the algorithms in which the amplified spontaneous emission (ASE) effect has not been considered. However, ASE is harmful in realization of a high-powered DPAL since the gain is very high. Usually, ASE becomes serious when the volume of the gain medium is large and the pump power is high. Basically, the conclusions we obtained in this study can be extended to other kinds of laser configurations.

1. Introduction

In the recent years, diode-pumped alkali laser (DPAL) has been extensively studied due to the potential for their excellent physical features [1–3]. The oscillator in a DPAL usually contains vapors of neutral alkali (K, Rb, Cs) and several kinds of buffer gases, such as helium and hydrocarbon with small molecular weight. Since the D2 ($n^2S_{1/2}\rightarrow n^2P_{3/2}$, where n = 4, 5, 6 for K, Rb, and Cs, respectively) and D1 ($n^2P_{1/2}\rightarrow n^2S_{1/2}$) transitions are spectrally close, the quantum defect in a DPAL is extremely small. In addition, DPAL has narrow linewidth, compact size, non-toxic system, etc [4,5]. With these advantages, DPAL has become one of the most hopeful candidates for realizing a high-powered laser system.

It is well–known that amplified spontaneous emission (ASE) can be a major source of upper laser level loss in high gain lasers [6]. The ASE will surely decrease the gain, and become more serious when the gain is higher. Thus the ASE must be considered in realization of a high-powered DPAL as the gain is very high. There have been few research groups referring the physical characteristics of the ASE in different kinds of laser systems including a DPAL system [7–9]. For the paper that studied ASE in an alkali laser, it mainly discussed a side-pumped alkali vapor amplifier [9].

In this paper, the ASE of an end-pumped DPAL is systemically studied by using a theoretical model. The influences of cell radius, cell length, and cell wall temperature on the optical-to-optical efficiency, fluorescence, and ASE have been evaluated.

2. Theoretical analyses

In this paper, we consider the configuration of a typical end-pumped continuous-wave DPAL with static media as schematically shown in Figure 1. After passing a polarized beam splitter (PBS), a pump beam with power of Pp enters into a cylindrical vapor cell with the length of L and the radius of R in which metallic cesium and buffer gases of ethane and helium have been beforehand sealed. The cavity consists of a high reflector with the reflectivity of 100% and an output coupler with the transmittance of 70%.

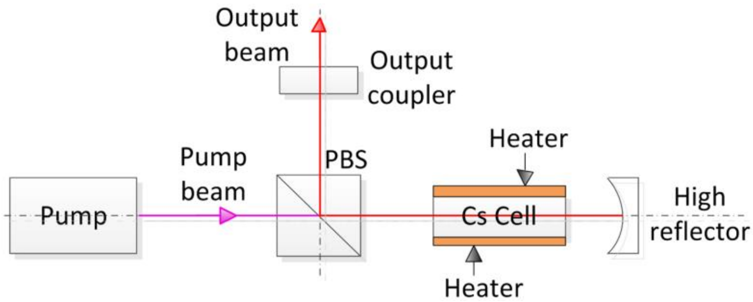

Figure 1. Schematic diagram of a static DPAL.

During the simulation, we made the following assumptions with purpose of the algorithm simplification:

(1) The transverse pump distribution holds out a Gaussian intensity profile and keeps unchanged along the optical axis;

(2) The temperature of every cylindrical annulus is a constant along the optical axis;

(3) The temperature distribution at the transverse section of a vapor cell is symmetrical.

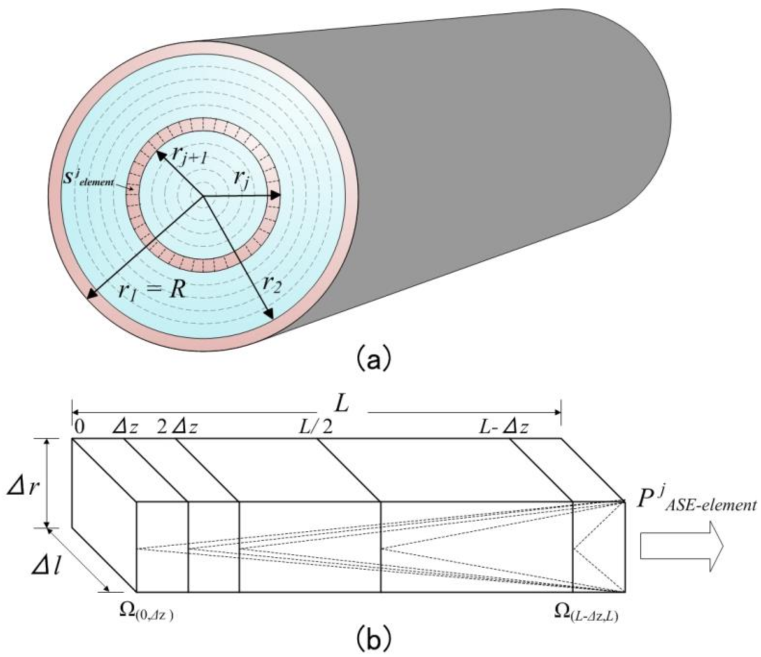

Figure 2. (a) Segmented configuration of a vapor cell and (b) schematic diagram of longitudinal ASE effect in a volume element in the *j*th cylindrical annulus.

In this model, we divide a cylindrical vapor cell into many coaxial cylindrical annuli, in which the temperature is treated as a constant along the optical axis as shown in Figure 2(a). Every cylindrical annulus is thought as both a heat source and a lasing source in the meantime. With respect to the heat transfer between the coaxial cylindrical annuli, we use the same theory of our previous paper [10–13]. To examine the effect of ASE and fluorescence of a DPAL, we make the second division of every cylindrical annulus. Each divided element has dimensions of $\Delta r \times \Delta l \times L$, where l is the perimeter of the jth annulus.

Figure 2(b) shows the schematic diagram of longitudinal ASE effect in an element. The element is further divided into many sub-segment with length of Δz. Each sub-segment has a solid angle relative to the end face of Ω. The ASE rate in an element is then expressed as [9]

$$\begin{aligned}\Gamma^j_{ASE-element} &= \frac{2P^j_{ASE-element}}{h\nu_{21}V^j_{element}} \\ &= \frac{2n^j_2}{\tau_{D_1}\left(n^j_2-n^j_1\right)}\frac{V^j_{element}}{\pi L^4}\int l(\lambda)\frac{\exp\left[\left(n^j_2-n^j_1\right)\sigma_{21}L\right]-1}{\sigma_{21}}d\lambda,\end{aligned} \tag{1}$$

where $P^j_{ASE-element}$ is the ASE power that emitted from an end of an element, $V^j_{element}$ is the volume of an element, n^j_i (i=1,2,3) is the number densities of the $6^2S_{1/2}$, $6^2P_{1/2}$, $6^2P_{3/2}$ energy level, τ_{D1} is the D_1 ($6^2P_{1/2}\rightarrow 6^2S_{1/2}$) radiative lifetime, σ_{21} is the atomic emission transverse section, $l(\lambda)$ is the normalized Lorentzian function that describes the spectral intensity distribution of spontaneous emission [14]

$$l(\lambda)=\frac{E}{\Delta\lambda}\cdot\frac{1}{1+\left(\dfrac{\lambda-\lambda_0}{\Delta\lambda/2}\right)^2}, \tag{2}$$

where E is the normalization constant, $\Delta\lambda$ is the full width at half-maximum of the emitted light, respectively. To simplify the algorithm of this model, the transverse ASE between the cylindrical annuli are not considered, and the transverse ASE in an element that induced by the other element in the same cylindrical annulus are assumed to have the same effect as a single element.

The appropriate laser rate equations of the *jth* cylindrical annulus (see Figure 2(a)) in a DPAL are

$$\begin{aligned}\frac{dn^j_1}{dt} &= -\Gamma^j_P+\Gamma^j_L+\Gamma^j_{ASE}+\frac{n^j_2}{\tau_{D_1}}+\frac{n^j_3}{\tau_{D_2}}, \\ \frac{dn^j_2}{dt} &= -\Gamma^j_L+\gamma_{32}\left(T_j\right)\left\{\left[n^j_3-n^j_2\right]-\left[2\exp\left(-\frac{\Delta E}{k_BT_j}\right)-1\right]n^j_2\right\}-\Gamma^j_{ASE}-\frac{n^j_2}{\tau_{D_1}}, \\ \frac{dn^j_3}{dt} &= \Gamma^j_P-\gamma_{32}\left(T_j\right)\left\{\left[n^j_3-n^j_2\right]-\left[2\exp\left(-\frac{\Delta E}{k_BT_j}\right)-1\right]n^j_2\right\}-\frac{n^j_3}{\tau_{D_2}},\end{aligned} \tag{3}$$

where Γ^j_P is the stimulated absorption transition rate caused by pump photons, Γ^j_L is the transition rate of laser emission, $\gamma_{32}\left(T_j\right)$ is the fine-structure relaxation rate, ΔE is the energy gap between the $^2P_{3/2}$ and $^2P_{1/2}$ levels with the value of 554 cm^{-1}, k_B is the Boltzmann constant, τ_{D2} is the D_2 ($6^2S_{1/2}\rightarrow 6^2P_{3/2}$) radiative lifetime, respectively.

3. Results and discussions

We first analyze the influence of the cell length on the optical-to-optical efficiency, fluorescence efficiency, and ASE efficiency. The cell radius, cell wall temperature, and pump power are set as 5 mm, 383 K, and 100 W, respectively. The results are shown in Figure 3. It can be seen that there is an optimal cell length corresponds to the maximal value of the optical-to-optical efficiency. For the curve of fluorescence, the fluorescence efficiency increases monotonously with the cell length. This is because that the longer cell length corresponds to the much more cesium atoms. On the contrary, the ASE efficiency decreases as the cell length increases. When the cell length exceeds 30 mm, the decrease of the ASE is not obvious.

IOP Conf. Series: Journal of Physics: Conf. Series **844** (2017) 012056 doi:10.1088/1742-6596/844/1/012056

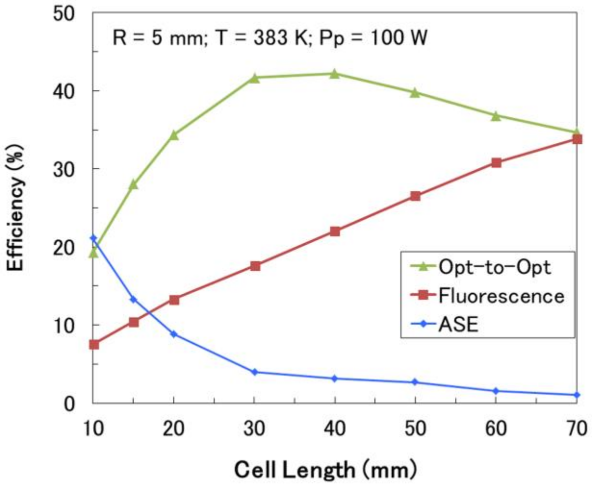

Figure 3. The influence of cell length on the optical-to-optical efficiency, fluorescence efficiency, and ASE efficiency with cell radius of 5 mm at cell wall temperature 383 K under 100 W-pumping.

Figure 4 shows the optical-to-optical efficiency, fluorescence efficiency, and ASE efficiency as a function of the cell radius, while the cell length, cell wall temperature, and pump power are set to be 40 mm, 383 K, and 100 W, respectively. It can be seen from Figure 4 that the cell radius has little influence on both the optical-to-optical efficiency and the fluorescence efficiency. The ASE increases obviously with the cell radius. Based on the results of Figure 3 and 4, the ASE effect might be suppressed to some extent by adjusting the cell dimensions.

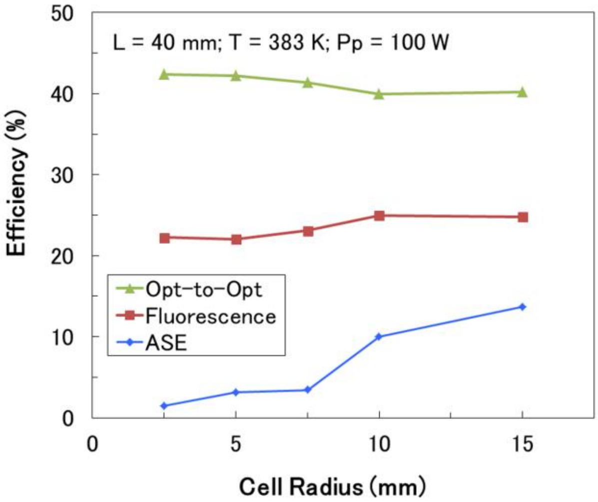

Figure 4. The influence of cell radius on the optical-to-optical efficiency, fluorescence efficiency, and ASE efficiency with cell length of 40 mm at cell wall temperature 383 K under 100 W-pumping.

Next, we analyze the influence of the cell wall temperature on the optical-to-optical efficiency, fluorescence efficiency, and ASE efficiency, respectively. The cell length, cell radius, and pump power are set to be 40 mm, 5 mm, and 100 W, respectively. Given a certain cell dimension, the total number of the cesium atom will change with the cell wall temperature. When the cell wall temperature is lower than the optimal value, the output power cannot achieve the peak value because of the shortage of the total number of cesium atoms. On the other hand, when the cell wall temperature becomes higher than the optimal value, the excessive cesium vapor will also lead to the reabsorption of the stimulated radiation in the cell. Since the fluorescence is in direct proportion to the cesium atom number, the fluorescence efficiency increases obviously with the cell wall temperature. For the case of ASE, its change is slightly.

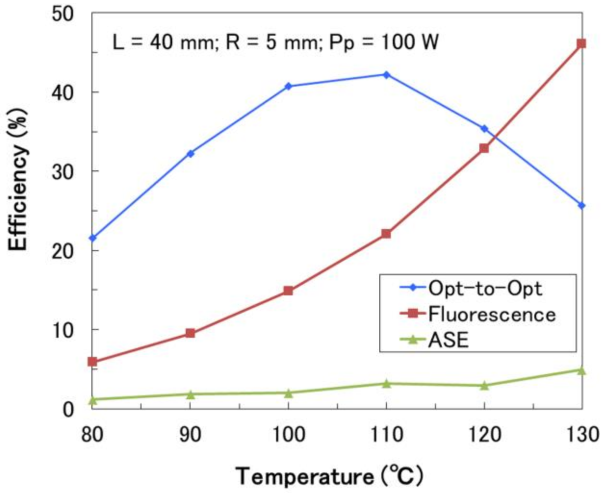

Figure 5. The influence of cell wall temperature on the optical-to-optical efficiency, fluorescence efficiency, and ASE efficiency with cell length and cell radius of 40 and 5 mm under 100 W-pumping, respectively.

In Figure 6, the output laser power, fluorescence power, and ASE power are given as a function of the pump power, respectively. The cell length, cell radius, and cell wall temperature are set to be 40 mm, 5 mm, and 383 K, respectively. It can be observed that the ASE and fluorescence power changed little with the pump power increases. This might could be ascribed to the cell dimension setting, suggesting that ASE can be suppressed to some extent.

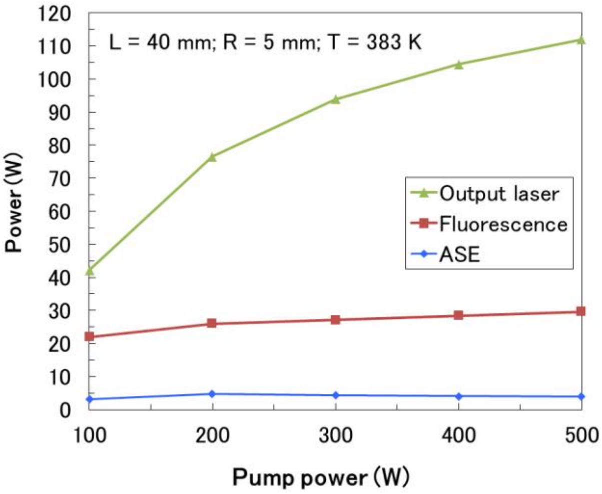

Figure 6. The influence of pump power on the power of output laser, fluorescence and ASE with cell length and cell radius of 40 and 5 mm at 383 K, respectively.

4. Summary

In this study, we develop a theoretical model to study a static-state DPAL by taking the process of amplified spontaneous emission (ASE) into account. The influences of the cell radius, cell length, and cell wall temperature on output features of a DPAL including ASE, fluorescence, and output power are systemically investigated. The results show that ASE can be effectively decreased by adjusting the cell dimension. And the output optical-to-optical efficiency can be optimized at the same time.

Acknowledgments

This work was supported by the National Natural Science Foundation of China under Grant No.61605178.

References

[1] Beach R J, Krupke W F, Kanz V K, and Payne S A 2004 *J. Opt. Soc. Am. B* **21** 2151
[2] Wang Y, Kasamatsu T, Zheng Y, Miyajima H, Fukuoka H, Matsuoka S, Niigaki M, Kubomura H, Hiruma T, an Kan H 2006 *Appl. Phys. Lett.* **88** 141112
[3] Krupke W F, 2012 *Prog. Quantum Electron.* **36** 4
[4] Zhdanov B V, Ehrenreich T, and Knize R J 2006 *Opt. Commun.* **260** 696
[5] Waichman K, Barmashenko B D and Rosenwaks S 2017 *J. Opt. Soc. Am. B* **34** 279
[6] Su H and Wang X 2012 *Proc. of SPIE* **8235** 82351Q
[7] Goren C, Tzuk Y, Marcus G and Pearl S 2006 *IEEE J. Quantum Electron.* **42** 1239
[8] Speiser J 2009 *J. Opt. Soc. Am. B* **26** 26
[9] Yang Z N, Wang H Y, Lu Q S, Hua W H, and Xu X J 2011 *Opt. Express* **19** 23118
[10] Han J H, Wang Y, Cai H, Zhang W, Xue L P and Wang H Y 2014 *Opt. Express* **22** 13988
[11] Han J H, Wang Y, Cai H, An G F, Zhang W, Xue L P, Wang H Y, Zhou J, Jiang Z G and Gao M 2015 *Opt. Express* **23** 9508
[12] An G F, Wang Y, Han J H, Cai H, Zhou J, Zhang W, Xue L P, Wang H Y, Gao M and Jiang Z G 2015 *Opt. Express* **23** 26414
[13] An G F, Wang Y, Han J H, Cai H, Wang S Y, Yu H, Rong K P, Zhang W, Xue L P, Wang H Y and Zhou J 2017 *Opt. Express* **25** 4335
[14] Copeland D A 2013 *Proc. of SPIE* **8599** 85991P